CHEMISTRY OF MATERIALS

Article

pubs.acs.org/cm

Multifunctional Colloids with Reversible Phase Transfer between Organic and Aqueous Media via Layer-by-Layer Assembly

Miseon Yoon, Jungkyu Choi,* and Jinhan Cho*

Department of Chemical & Biological Engineering, Korea University, Anam-dong, Seongbuk-gu, Seoul 136-713, South Korea

Supporting Information

ABSTRACT: We report the successful multifunctional colloids that enable reversible phase transfer between organic and aqueous phases via layer-by-layer (LbL) assembly. These colloids exhibited a high level of dispersion stability in a variety of solvents ranging from nonpolar to aqueous media, based on the type of outermost layer adsorbed onto the colloids. Hydrophobic nanoparticles (NPs) synthesized using carboxylic acid or ammonium moiety-based ligands (i.e., oleic acid or tetraoctylammonium) in a nonpolar solvent (toluene, hexane, or chloroform) were directly deposited onto dendrimer-coated SiO_2 colloids via ligand exchange between the hydrophobic ligands and the amine-functionalized dendrimers in the same organic solvent. Additionally, these hydrophobic NPs were adsorbed onto the colloids forming the densely packed layer structure that could not be easily achieved by conventional electrostatic LbL assembly. The subsequent adsorption of amine-functionalized dendrimers onto hydrophobic NP-coated colloids led to well-dispersed colloids in aqueous media as well as alcohol solvent and possibly induced the deposition of electrostatic LbL-assembled films, such as (cationic Au_{NP}/anionic polyelectrolyte (PE))$_n$ or (cationic PE/anionic enzyme)$_n$ multilayers. Furthermore, the additional deposition of ligand exchange-induced multilayers (i.e., (dendrimer/hydrophobic NP)$_n$) onto electrostatic multilayer-coated colloids produced colloids with highly dispersible properties in organic media. Given that previous approaches to the reversible phase transfer of colloids have depended on the physicochemical properties of selective ligands under limited and specific conditions, our approach may provide a basis for the design and exploitation of high-performance colloids with tailored functionality in a variety of solvents.

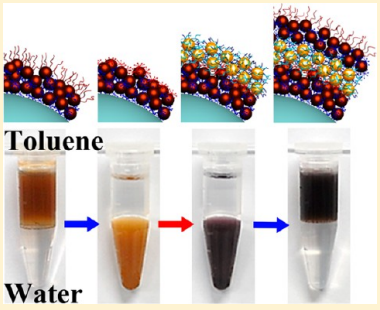

KEYWORDS: *multifunctional colloids, phase transfer, layer-by-layer assembly, multilayers, magnetic nanoparticles*

INTRODUCTION

Coated colloidal particles, which can be prepared using layer-by-layer (LbL)-assembled[1−14] organic/organic or organic/inorganic nanoparticle (NP) multilayers, are promising for a wide range of applications, such as photonic materials,[15−17] surface-enhanced Raman scattering,[18] and chemical and biological sensing,[19] because the properties and performances of core−shell-type composite colloids can be altered or enhanced through the coating of the colloidal cores with shells that have desirable functionalities.

Two important requirements for obtaining high-performance functional colloids and for promoting their use in a wide range of applications need to be met: the dense adsorption of functional components onto the colloids and sufficient dispersion stability of the resultant colloids in a variety of solvents. To date, studies have mainly focused on electrostatic LbL assembly, which can produce colloidal coatings without agglomeration in aqueous media.[1−24] However, in the case of the adsorption of electrostatically charged inorganic NPs (i.e., small colloids) onto large colloids, the low packing density of the NPs due to the electrostatic repulsion between similarly charged NPs[21−23] can have an unfavorable effect on the performance of the functional colloids. In addition, functional colloids prepared via electrostatic LbL assembly cannot be directly utilized in petrochemical industries, which require high levels of dispersion in organic media (mainly nonpolar solvents). Although the preparation of LbL (polymer/inorganic NP)$_n$ multilayer-coated SiO_2 colloids using a nucleophilic substitution (NS) between an amine-functionalized polymer and the bromo group-containing stabilizer of an inorganic NP in organic media has recently been reported,[25] our previous approach based on NS reaction-induced LbL assembly led to the NPs being significantly destabilized in aqueous media, which caused colloidal aggregation.

Several methods used to enhance the dispersion stability of colloids in organic and aqueous media are based on the use of selective ligands with unique physicochemical properties. For example, a variety of colloids, such as Ag, Au, $CoFe_2O_4$, CdSe/ZnS, or SiO_2, can undergo reversible phase transfer with an aid of selective ligands in controlled environments (e.g., pH variation, temperature changes, or irradiation with UV light).[26−30] However, these approaches limit the integration of functionalities into the composite colloids of interest. Therefore, our goal is to develop a method for the dense adsorption of a variety of functional NPs onto one large colloid while retaining the ability of the colloid to simultaneously

Received: January 18, 2013
Revised: March 18, 2013
Published: March 20, 2013

disperse in a variety of solvents (or to reversibly phase transfer between organic and aqueous media) for use in a wide range of potential applications.

In this study, we report the preparation of multifunctional colloids with reversible phase transfer between organic and aqueous media via LbL assembly (Figure 1). These colloids

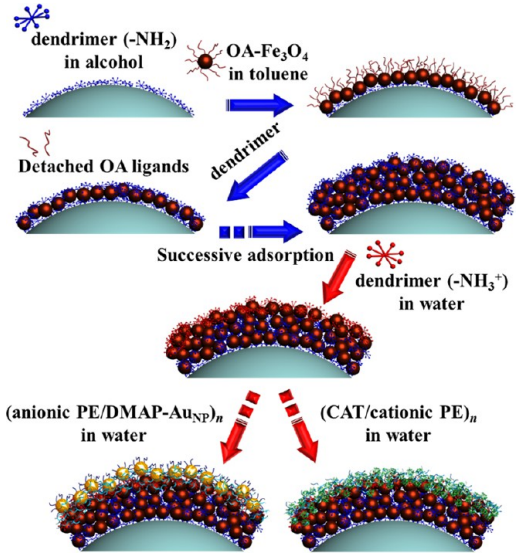

Figure 1. Schematic for the preparation of multifunctional colloids via ligand exchange-induced (in organic media) and electrostatic LbL assembly (in aqueous media).

were highly dispersible in a variety of solvents that ranged from nonpolar (toluene or hexane) to aqueous media. For this study, magnetically inducible colloids, which were used as a model system, were first prepared using the ligand exchange between hydrophobic NPs in a nonpolar solvent and amine-functionalized dendrimers in alcohol; this approach significantly increased the adsorbed amount of hydrophobic NPs per layer. It is here highlighted that the densely packed structure of hydrophobic NPs shown in our system has not been easily achieved using electrostatic LbL assembly approaches. In the case of anionic Fe_3O_4 NP-multilayered colloids based on electrostatic LbL assembly, the surface coverage of anionic Fe_3O_4 NP layer was extremely low compared to that of hydrophobic Fe_3O_4 NP layer. Additionally, the oleic acid (OA) or tetraoctylammonium (TOA) ligands bound to the surface of the Fe_3O_4, Ag, or Au NPs could be replaced by the dendrimers because of the high affinity between the amine group-containing dendrimer and the metal oxide or metal NP, which allowed the vertical growth of LbL-assembled polymer/hydrophobic NP multilayers.[31−34]

The dendrimer layer deposited as an outermost layer on these colloids gave them high dispersion stability in aqueous media as well as alcohol solvent, which enabled the phase transfer from organic to aqueous media and induced the electrostatic LbL assembly of functional multilayers. Furthermore, the successive adsorption of ligand exchange-induced multilayers onto the electrostatic multilayer-coated colloids resulted in the phase transfer from the aqueous solution back to the organic medium. To the best of our knowledge, the colloids, which enable reversible phase transfer and densely packed hydrophobic NP layers via LbL assembly, have not been previously reported. Considering the fact that hydrophobic ligands (e.g., carboxylic acid or ammonium moieties) bound to the surface of metal or metal oxide NPs (e.g., OA−Fe_3O_4 NP, OA−Ag_{NP}, or TOA−Au_{NP}) can easily be replaced by amine-functionalized polymers via ligand exchange reaction, we believe that our approach may provide a basis for designing and exploiting smart functional colloids that can be used in a variety of solvents.

EXPERIMENTAL SECTION

Materials. Poly(amidoamine) dendrimer (core type: ethylene diamine), OA, oleylamine, 1,2-hexadecanediol, benzyl ether, poly(allylamine hydrochloride) (PAH), tetraoctylammonium bromide (TOA), $NaBH_4$, and catalase enzymes (CAT) (from bovine liver) were purchased from Sigma Aldrich. OA−Fe_3O_4 NP with approximately 5 nm diameter was synthesized in toluene, as reported previously by Sun et al. $Fe(acac)_3$ (2 mmol), 1,2-hexadecanediol (10 mmol), OA (5 mmol), oleylamine (6 mmol), and benzyl ether (20 mL) were mixed and stirred under a flow of nitrogen. The mixture was heated to 200 °C for 2 h and heated to reflux (approximately 300 °C) for 1 h under a blanket of nitrogen. The black mixture was cooled to room temperature by removing the heat source. Ethanol (40 mL) was added to the mixture under ambient conditions, and a black material was precipitated and separated via centrifugation. The black product was dissolved in hexane or toluene in the presence of OA (0.05 mL) and oleylamine (0.05 mL). Centrifugation (6000 rpm, 10 min) was applied to remove the undispersed residue. A black−brown toluene dispersion of 5.1 nm sized Fe_3O_4 NPs stabilized by OA was produced, and its concentration was adjusted to 0.5 wt % in toluene.

Anionic Fe_3O_4 NPs were prepared as reported by other research groups.[35,36] Briefly, 1 M $FeCl_3$ (20 mL) and $FeSO_4$ (5 mL) in 2 M HCl were added to 0.7 M NH_4OH (250 mL) with mechanical stirring for 1 h. The black solid powder was separated with the aid of a magnet. The product was then redispersed in aqueous solution, and subsequently 1 M tetramethylammonium hydroxide solution (10 mL) was added. Finally, its concentration was adjusted to 0.5 wt %.

The 4-dimethylaminopyridine (DMAP)-stabilized Au_{NP} dispersion was synthesized, as reported previously.[37] Thirty millimolar aqueous $HAuCl_4$ (30 mL) was added to a 25 mM solution of TOABr in toluene (80 mL). The transfer of the $HAuCl_4$ to the toluene phase can be clearly seen within a few seconds. A 0.4 M $NaBH_4$ solution (25 mL) was added to the mixture. After 10 min, the separated aqueous phase was removed and the toluene phase, containing the reduced Au NPs, was subsequently washed with 0.1 M H_2SO_4, 0.1 M NaOH, and H_2O (three times). For transfer from toluene to the aqueous phase, an aqueous 0.1 M DMAP solution (80 mL) was added to the toluene solution (80 mL) containing TOA−Au_{NP}. After 24 h, the Au NPs dispersed in toluene were completely phase-transferred to the aqueous phase and the separated toluene phase was removed. The resulting Au NPs dispersed in the aqueous phase were stabilized by the DMAP ligands.

Build-Up of LbL Multilayers onto Colloids. The (dendrimer/OA−Fe_3O_4 NP)$_n$ multilayer-coated SiO_2 colloids were prepared as follows: A concentrated dispersion (6.4 wt %) of anionic 585 nm sized SiO_2 colloids (100 μL) was diluted to 0.5 mL with deionized water. After centrifugation (radius rotation ~5.5 cm) at 8000 rpm for 5 min (Micro 17TR, Hanil Science Industrial Co. Ltd.) of the colloidal solution, the supernatant water was removed, and then dendrimer ethanol

dx.doi.org/10.1021/cm400207d | Chem. Mater. 2013, 25, 1735−1743

solution (0.5 mL) of 1 mg·mL^{-1} was added to the colloids, which was followed by ultrasonication and sufficient adsorption time (10 min). Excess dendrimer was removed by three centrifugation (8000 rpm, 5 min)/washing cycles. Then 5 mg·mL^{-1} OA−Fe_3O_4 NPs/toluene (0.5 mL) was added to prepare multilayers on the dendrimer-coated SiO_2 colloids and the excess OA−Fe_3O_4 NPs was removed after deposition for 10 min by three centrifugation steps as described above. Then 1 mg·mL^{-1} dendrimer/ethanol (0.5 mL) was deposited onto the OA−Fe_3O_4 NP-coated colloids under the same conditions. The above process was repeated until the desired number of layers was deposited on the colloidal SiO_2. Subsequently, electrostatic CAT/PAH or PAA/DMAP−Au_{NP} multilayers were deposited onto (dendrimer/OA−Fe_3O_4 NP)$_n$/dendrimer multilayer-coated SiO_2 colloids in aqueous solution. For this approach, the concentrations of CAT, PAH, and PAA were adjusted to 1 mg·mL^{-1}. The procedure for the build-up of electrostatic multilayers was exactly the same as that for (dendrimer/OA−Fe_3O_4 NP)$_n$ multilayers.

Measurements. UV−vis spectra were obtained using a UV−vis spectrometer (Lambda 35, Perkin-Elmer). A QCM device (QCM200, SRS) was used to examine the mass of the material deposited after each adsorption step. The resonance frequency of the QCM electrodes was approximately 5 MHz. The adsorbed mass of dendrimer and OA−Fe_3O_4 NPs, Δm, was calculated from the change in QCM frequency, ΔF, using the Sauerbrey equation:[38]

$$\Delta F(\mathrm{Hz}) = -\frac{2F_0^2}{A\sqrt{\rho_q \mu_q}} \cdot \Delta m$$

Here, F_0 (~5 MHz) is the fundamental resonance frequency of the crystal, A is the electrode area, and ρ_q (~2.65 g·cm^{-2}) and μ_q (~2.95 × 10^{11} g·cm^{-2}·s^{-2}) are the shear modulus and density of quartz, respectively. This equation can be simplified as follows:

$$\Delta F(\mathrm{Hz}) = -56.6 \times \Delta m_A$$

where Δm_A is the mass change per quartz crystal unit area in μg·cm^{-2}. Vibrational spectroscopic characterization of Au-coated Si substrates was carried out using ATR-FTIR spectroscopy (Spectrum 400, Perkin-Elmer) in the ATR mode. The magnetism of (dendrimer/OA−Fe_3O_4 NP)$_n$ multilayer-coated colloids was measured using a SQUID magnetometer (MPMS5). The surface morphology and the size of multilayer-coated colloids were obtained from Hitachi S-4300 FE-SEM. We also determined the colloidal size from a randomly selected sample of 20 colloids with the same bilayer number and layer species.

RESULTS AND DISCUSSION

Chemical Analysis of Ligand-Exchange Reaction. OA−Fe_3O_4 NPs, with diameters of approximately 5.1 ± 0.5 nm (see Supporting Information, Figure S1), prepared in toluene were directly deposited onto substrates coated with poly(amidoamine) dendrimers in the form of an amine-functionalized polymer. The OA ligands, which are loosely bound to the surfaces of the Fe_3O_4 NPs, can be easily replaced by the dendrimers via ligand exchange because of the high affinity between the Fe_3O_4 NPs and the amine groups of the dendrimers. Although the −COO^- group acts either as a chelating ligand that binds to Fe via two O atoms, or as a monodentate ligand that links to Fe via only one O atom,[39,40] the carboxylate-based surfactants around each iron oxide NPs can be replaced by other similarly structured acids or by surfactants with a functional group that has a high affinity for Fe.[41] This ligand exchange between the OA ligands bound to Fe_3O_4 NPs and the dendrimers was confirmed using Fourier-transform infrared spectroscopy (FTIR) in the attenuated total reflectance (ATR) mode (Figure 2). The C−H stretching

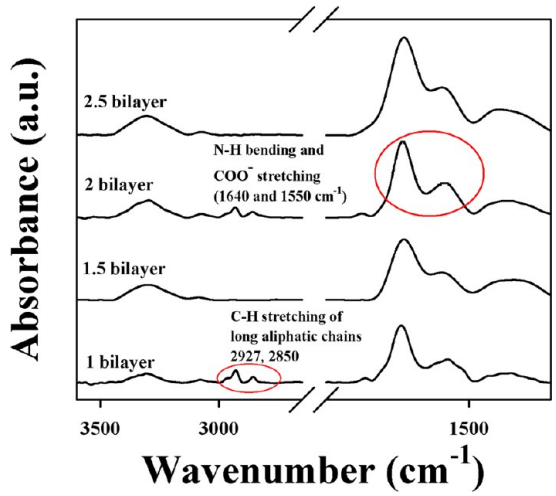

Figure 2. ATR-FTIR spectra of ligand exchange-induced (dendrimer/OA−Fe_3O_4 NP)$_n$ multilayer films as a function of bilayer number (n). The weak absorbance peak at 1710 cm^{-1} was derived from the C═O stretch of excess OA in the outermost OA−Fe_3O_4 NP layer (*i.e.*, 1 and 2 bilayered films).

(2850 and 2927 cm^{-1}), COO^- asymmetric (1550 cm^{-1}) and symmetric stretching (1640 cm^{-1})[40] of the OA ligand bound to Fe_3O_4 NPs, which contains a carboxylic acid group and long aliphatic chains, and the N−H stretching (3300 cm^{-1}) of the amine groups were observed for the OA−Fe_3O_4 NPs and the dendrimers (see Supporting Information, Figure S2). It was reported by Zhang et al. that the COO^- stretch bands at 1640 cm^{-1} appeared instead of the C═O stretch band (1710 cm^{-1}) by the carboxyl group when the OA ligands are bound to the surface of Fe_3O_4 NPs.[42] Additionally, the N−H bending modes (1550 and 1640 cm^{-1}) of the dendrimer are almost overlapped with −COO^- stretching of OA ligands bound to Fe_3O_4 NPs. Therefore, the two absorption peaks (1550 and 1640 cm^{-1}) attributable to −COO^- stretching of OA and N−H bending of the dendrimer were due to substrate/(dendrimer/OA−Fe_3O_4 NP)$_1$.

In the case of the subsequent adsorption of a dendrimer layer onto the OA−Fe_3O_4 NP-coated film, the strong absorption intensities of the peaks for C−H stretching (2850 and 2927 cm^{-1}), which were due to the OA ligand as mentioned above (see Supporting Information, Figure S2), significantly decreased during the deposition. This phenomenon indicates that the OA ligands on the surface of the top Fe_3O_4 layer are replaced by the dendrimer layer when the outermost layer is changed from OA−Fe_3O_4 to a dendrimer layer via the sequential adsorption process. When the outermost layer is then changed from the dendrimers to OA−Fe_3O_4, the absorption peaks that originate from the OA ligands (i.e., C−H stretching) are again observed. The absorption intensities of the peaks for carboxylate (1550 and 1640 cm^{-1}) of OA−Fe_3O_4 NP and N−H stretching (3300 cm^{-1}) of dendrimer increased due to the successive adsorption process. These results

dx.doi.org/10.1021/cm400207d | *Chem. Mater.* 2013, 25, 1735−1743

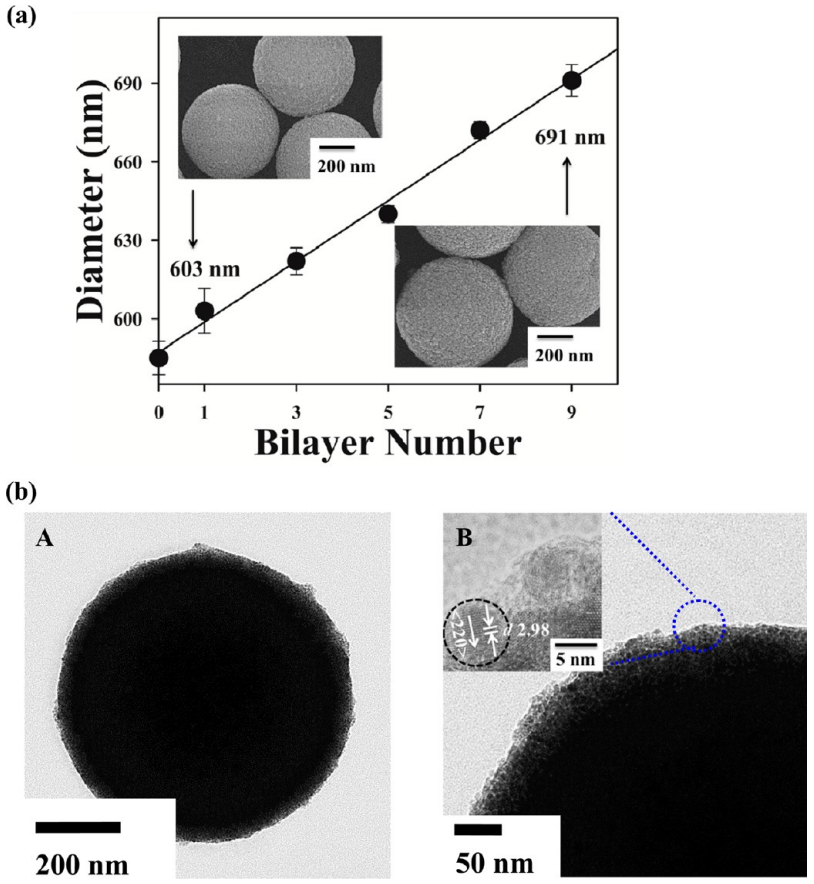

Figure 3. (a) The size change of (dendrimer/OA−Fe_3O_4 NP)$_n$ multilayer-coated SiO_2 colloids with increasing bilayer number (n). The insets show FE-SEM images of (dendrimer/OA−Fe_3O_4 NP)$_n$ multilayer-coated SiO_2 colloids (n = 1 and 9). The colloidal size was determined from FE-SEM images. (b) HR-TEM images of (dendrimer/OA−Fe_3O_4 NP)$_9$ multilayer-coated SiO_2 colloids. The image on the right (B) is magnified two times the image on the left (A).

demonstrated that the driving force between the dendrimers and OA−Fe_3O_4 NPs is the ligand exchange reaction between the OA and the NH_2 groups. Notably, OA−Ag_{NP} and TOA−Au_{NP} could also be LbL-assembled with an amine-functionalized polymer using the ligand exchange approach (see Supporting Information, Figure S3).

On the basis of these results, 5.1 nm OA−Fe_3O_4 NPs were deposited onto dendrimer-coated SiO_2 colloids with diameters of 585 ± 5 nm, and dendrimers were subsequently adsorbed onto the OA−Fe_3O_4 NP-coated colloids. As shown in Figure 3a, the (dendrimer/OA−Fe_3O_4 NP)$_n$ multilayer-coated colloids increased in diameter from approximately 585 ± 5 to 691 ± 6 nm without any colloidal aggregation when the bilayer number (n) of multilayers was increased from 0 to 9. The uniform and dense coating of the nanocomposite multilayers [i.e., (dendrimer/OA−Fe_3O_4 NP)$_9$ multilayers] was confirmed using high-resolution transmission electron microscopy (HR-TEM), as shown in Figure 3b. Additionally, the dispersion stability of (dendrimer/OA−Fe_3O_4 NP)$_n$ multilayer-coated colloids in various solvents strongly depends on the deposited top layer (see Supporting Information, Figure S4). If the dendrimer was deposited as a top layer, these colloids could well disperse in polar organic solvent such as ethanol or methanol. On the other hand, if OA−Fe_3O_4 NP layer was used as a top layer, the formed colloids could be well dispersed in nonpolar solvent such as toluene, hexane, or chloroform. However, electrostatically charged colloids exhibited poor dispersion stability, inducing precipitation in organic media.

Although the quantitative density of the OA−Fe_3O_4 NPs on the colloidal substrate could not be precisely determined, the frequency change in a quartz-crystal microbalance (QCM) with a flat Au electrode (see Supporting Information, Figure S5) enabled the estimation of the amount of OA−Fe_3O_4 NPs adsorbed onto the 585 nm colloids, which had surface areas of approximately 1.08×10^{-8} cm^2. The average amount of adsorbed OA−Fe_3O_4 NPs calculated using the QCM frequency change was approximately 1307 ng·cm^{-2} (see Experimental Section). Given that the density and volume of the 5.1 nm OA−Fe_3O_4 NPs were 5.17 g·cm^{-3} and 6.95×10^{-20} cm^3, respectively, the mass of one NP was approximately 3.59×10^{-10} ng; therefore, the number of OA−Fe_3O_4 NPs in a single layer adsorbed onto a colloid with a surface area of approximately 1.08×10^{-8} cm^2 was approximately 38 900 NPs per SiO_2 colloid.

Magnetic Properties of Iron Oxide NP-Based Colloids. The magnetization of the (dendrimer/OA−Fe_3O_4 NP)$_4$ multilayer-coated colloids was examined using superconducting quantum interference device (SQUID) magnetometry. The magnetization curves of the multilayered films that were measured at room temperature (T = 298 K) were reversible and did not exhibit any coercivity, remanence, or hysteresis, which suggests typical superparamagnetic behavior (Figure 4a). At liquid-helium temperature (T = 5 K), the magnetization

dx.doi.org/10.1021/cm400207d | Chem. Mater. 2013, 25, 1735−1743

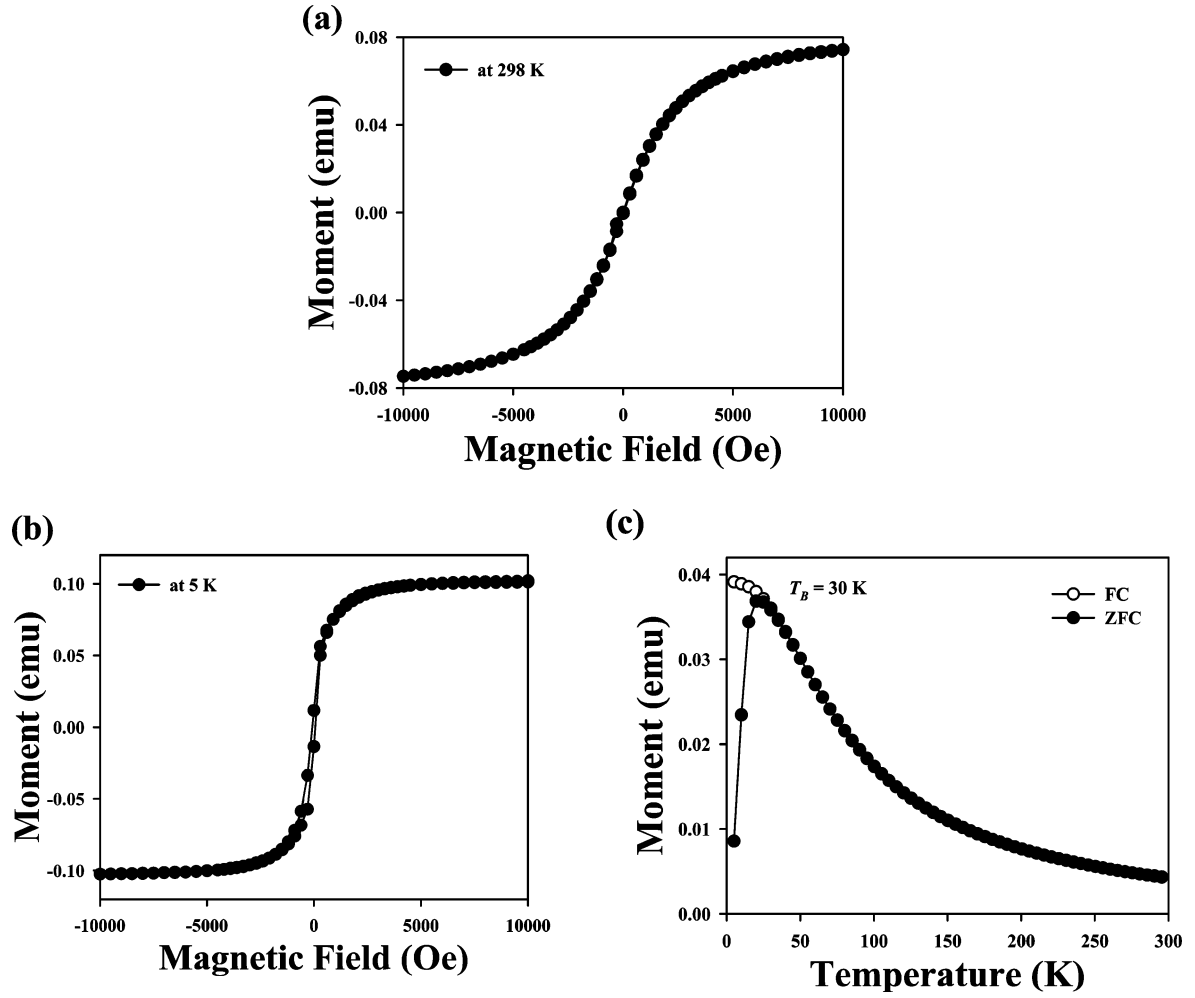

Figure 4. Magnetic curves of (dendrimer/OA–Fe_3O_4 NP)$_4$ multilayer-coated SiO_2 colloids measured at (a) 298 K and (b) 5 K. (c) The temperature dependence of zero-field-cooling (ZFC) and field-cooling (FC) magnetization measured at 150 Oe.

curves exhibited a loop shape with distinct hysteresis in the two sweeping directions, which is typically observed for ferromagnets with frustrated superparamagnetic properties (Figure 4b).

We also investigated the temperature dependence of the magnetization of the dendrimer/OA–Fe_3O_4 NP multilayer-coated colloids from 300 to 5 K using an applied magnetic field of 150 Oe (Figure 4c). The blocking temperature,[43,44] where some deviation between the zero-field-cooling (ZFC) and field-cooling (FC) magnetizations begins to be exhibited, was approximately 30 K for the nanocomposite multilayers that were coated with approximately 5 nm OA–Fe_3O_4 NPs. The blocking temperature of isolated Fe_3O_4 NPs with diameters of 5 nm has been reported to be approximately 30 K.[45] The blocking temperature of an Fe_3O_4 NP array has also been reported to shift to significantly higher temperatures when the isolated array was changed into a 3D NP array because of the relatively strong dipole interactions between the magnetic moments of the individual particles.[46] In this previous study, the Langmuir–Blodgett method was used to build the NP multilayers without the use of insulating polymers.

On the basis of these previous findings, our results suggest that the dendrimer/OA–Fe_3O_4 NP multilayers could preserve the intrinsic magnetic properties of the isolated NPs because the interposed dendrimer layers separate the NPs and, thus, effectively block the dipole interactions between the magnetic NPs. In the case of the colloids that were coated with alternating layers of anionic Fe_3O_4 NPs with a broad size distribution (approximately 8.4 ± 2.6 nm), which were synthesized in an aqueous solution and cationic PAH (see Supporting Information, Figure S6), the packing density of the anionic Fe_3O_4 NPs was extremely low due to the electrostatic repulsion between the aqueous NPs with the same charge (Figure 5); consequently, we did not obtain meaningful magnetization curves for these colloidal particles.

Water-Dispersible Enzymatic Colloids with Hydrophobic Iron Oxide NP layers. On the basis of these results, we prepared multifunctional colloids (i.e., magnetically inducible enzymatic or metallic colloids) with good dispersion in an aqueous solution and in organic media. Although the ligand exchange multilayer-coated colloids were prepared via the alternating deposition of OA–Fe_3O_4 NPs (in toluene) and dendrimers (in alcohol) in organic media, the colloids that were coated with an outermost dendrimer layer [i.e., SiO_2/(dendrimer/OA–Fe_3O_4 NP)$_n$/dendrimer] could be well dispersed in aqueous media (i.e., deionized water with a pH of 5.8) without any colloidal aggregation. This phenomenon is due to the amine protonation of the dendrimers, which induces electrostatic repulsion between neighboring positively charged colloids in aqueous media. It was reported by Choi and Rubner that the pK_a value (i.e., the pH value at which 50% of the

dx.doi.org/10.1021/cm400207d | *Chem. Mater.* 2013, 25, 1735–1743

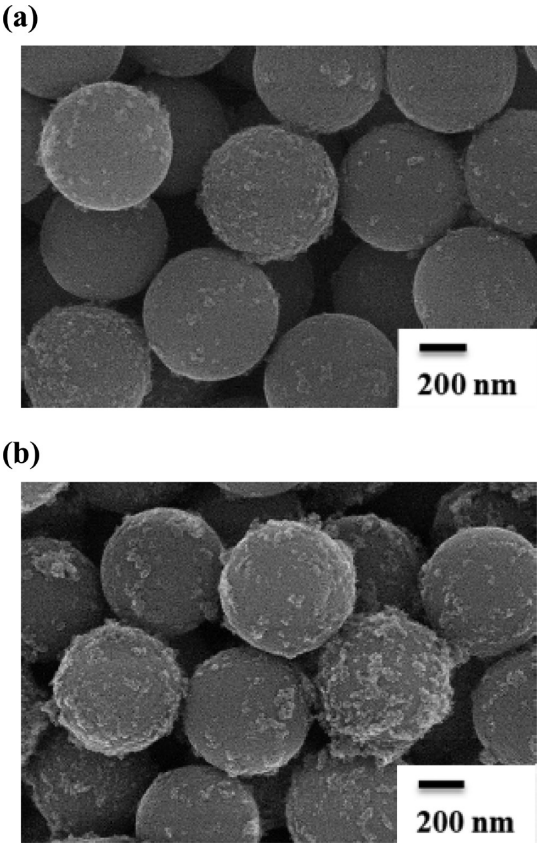

Figure 5. SEM images of (a) (PAH/anionic Fe_3O_4 NP)$_1$ and (b) (PAH/anionic Fe_3O_4 NP)$_3$ multilayer-coated SiO_2 colloids. The (PAH/anionic Fe_3O_4 NP)$_n$ multilayers assembled onto colloids were prepared from 1 mg·mL^{-1} PAH aqueous solution containing 0.2 M NaCl and 2 mg·mL^{-1} anionic Fe_3O_4 aqueous solution. The deposition time for PAH and anionic Fe_3O_4 NPs was adjusted to 30 and 60 min, respectively.

functional groups of a polymer are ionized) of an amine-functionalized polymer, such as PAH, was approximately 8.0–9.0.[47] Furthermore, this colloidal dispersion in an aqueous solution indicates that traditional electrostatic multilayers could be deposited onto ligand exchange multilayer-coated colloids.

To confirm our hypothesis, negatively charged CAT and positively charged PAH were used in an aqueous solution at pH 9 for the adsorption of electrostatic multilayers onto the colloids that were coated with an outermost dendrimer layer [i.e., SiO_2/(dendrimer/OA–Fe_3O_4 NP)$_4$/dendrimer]. CAT, which has an isoelectric point of 5.6, is well-known to have an overall positive charge at pH < 5.6 and a negative charge at pH > 5.6.[48−52] First, electrophoresis experiments were performed to monitor the CAT/PAH multilayer growth on the ligand exchange multilayer-coated colloids because the zeta (ξ) potential has been shown to be an indicator of stable growth for electrostatic multilayer films (Figure 6a). When the colloids with an outermost dendrimer layer, which were prepared in an organic solvent, were dispersed in a pH 9.0 aqueous solution, the initial zeta potential of the colloids was approximately +29.2 ± 0.7 mV. However, when CAT and PAH were alternately adsorbed onto the colloids with an outermost dendrimer layer, the zeta potential of anionic CAT and cationic PAH periodically and uniformly oscillated from −37.3 ± 1.1 to +23.5 ± 1.4 mV, which indicates stable electrostatic multilayer growth. The uniform adsorption of (CAT/PAH)$_{n=1-4}$ multilayers onto the ligand exchange multilayer-coated colloids was confirmed by SEM experiments (Figure 6b).

On the basis of the stable growth of the CAT/PAH multilayers, we investigated the functionality of the colloids coated with ligand exchange and electrostatic multilayers. As shown in Figure 5c, the ligand exchange multilayer-coated colloids that were dispersed in toluene phase transferred to aqueous media because of the successive adsorption of electrostatic CAT/PAH multilayers, and the resulting colloids accumulated near a handheld magnet that was placed near the plastic tube. The magnetically responsive colloids were expected to exhibit electrocatalytic behavior toward H_2O_2 because CAT, which has iron-containing heme groups, is an efficient catalyst for H_2O_2.[48−53] Figure 5c shows the catalytic response of indium tin oxide (ITO) electrodes modified with (CAT/PAH)$_3$/ligand exchange multilayer-coated colloids in pH 7.0 phosphate-buffered saline for scan rates increased from 50 to 250 mV·s^{-1} over the potential range of 0 to −0.8 V. The catalytic current increased significantly with increasing scan rate, which is characteristic of an electrocatalytic reduction process. The bare ITO electrode exhibited no current response within this potential range.

Iron heme CAT (i.e., CAT–Fe^{III}) has been reported to first form reactive oxidants with H_2O_2, including a cation radical on the heme porphyrin [(CAT–Fe^{IV}=O)$^{\bullet}$].[49] (CAT–Fe^{IV}=O)$^{\bullet}$ then accepts an electron from H_2O_2 to form a nonradical compound [(CAT–Fe^{IV}=O)], which causes the oxidation of H_2O_2. This nonradical compound can accept a second electron to regenerate the iron heme CAT. The catalytic H_2O_2 current is attributed to the reduction of (CAT–Fe^{IV}=O)$^{\bullet}$.[49,53] However, all the CAT/PAH multilayer domains deposited onto the magnetic colloids are not electrocatalytically active because of the limited electron transfer distance between the CAT molecules and the electrode surface. Therefore, we conclude that the electrocatalytic behaviors of enzymatic and magnetic colloids are mainly due to the CAT multilayers that are near the electrodes. These results demonstrate that the combination of hydrophobic and hydrophilic multilayers with different functionalities could provide a strategy for the design of colloids with desirable multifunctionality.

Water-Dispersible Colloids with Magnetic and Surface Plasmon Resonance Properties. Our approach can be extended to noble-metal NP-coated colloids that exhibit a magnetic response, which enables the reversible phase transfer of large functional colloids between organic and aqueous media. For this study, cationic Au_{NPs} stabilized by 4-dimethylaminopyridine (DMAP) ligands (DMAP–Au_{NPs}),[37] which display a surface plasmon absorption peak at 520 nm, were alternately LbL-assembled with anionic poly(acrylic acid) (PAA) at pH 4 onto colloids that were coated with an outermost dendrimer layer [i.e., SiO_2/(dendrimer/OA–Fe_3O_4 NP)$_{4.5}$]. Similar to the (CAT/PAH)$_n$ multilayer-coated colloids shown in Figure 5a, these colloids exhibited zeta potentials that periodically changed from −15.2 ± 1.1 to +32.9 ± 1.8 mV as PAA and DMAP–Au_{NPs} were alternately deposited onto the dendrimer-coated colloids (see Supporting Information, Figure S7).

This approach, in which electrostatic PAA/DMAP–Au_{NP} multilayers were deposited onto (dendrimer/OA–Fe_3O_4 NP)$_{4.5}$-coated colloids, produced a more rugged structure without inducing colloidal aggregation (Figure 7a). Furthermore, by increasing the number of PAA/DMAP–Au_{NP} bilayers (n) from 1 to 5, the surface plasmon absorption peak due to the DMAP–Au_{NPs} became more evident and notably red-shifted to

dx.doi.org/10.1021/cm400207d | Chem. Mater. 2013, 25, 1735−1743

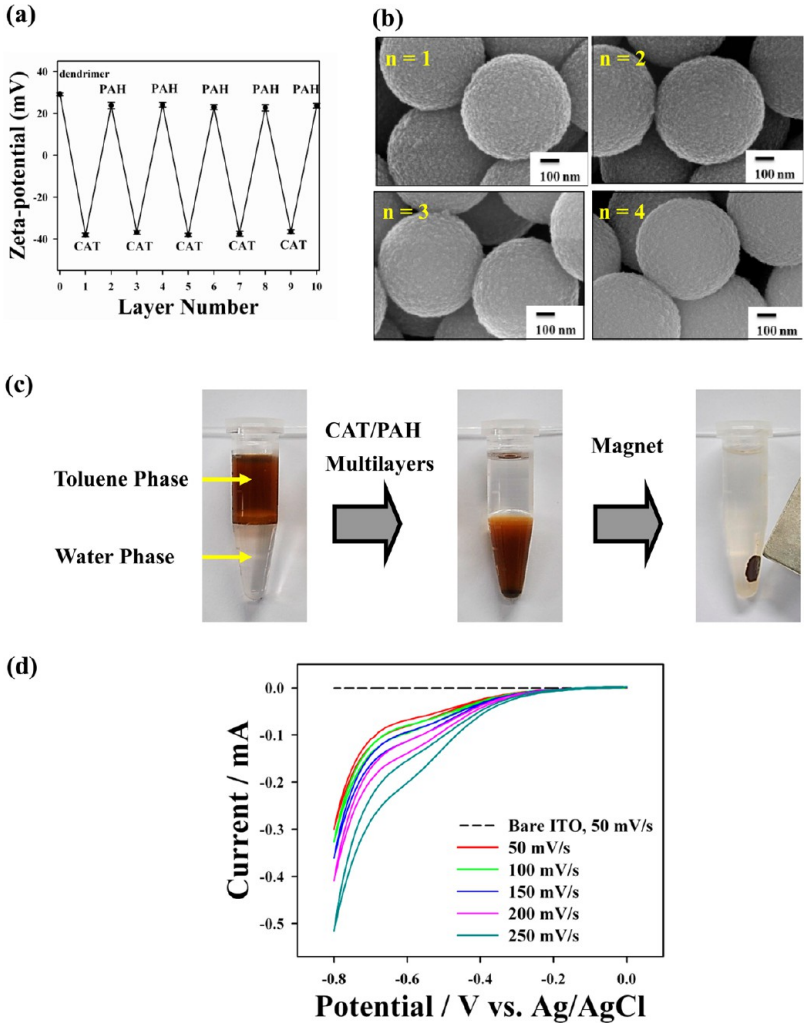

Figure 6. (a) Periodic change in zeta potential values occurring with the alternating deposition of anionic catalase (at pH 9) and cationic PAH (at pH 9) onto the (dendrimer/OA−Fe_3O_4 NP)$_{4.5}$ multilayer-coated SiO_2 colloids with an outermost dendrimer layer. (b) SEM images of (dendrimer/OA−Fe_3O_4 NP)$_{4.5}$/(CAT/PAH)$_n$ multilayer-coated colloids (n = 1, 2, 3, and 4). (c) Phase transfer of (dendrimer/OA−Fe_3O_4 NP)$_4$ multilayer-coated colloids from toluene to aqueous solution after the deposition of (CAT/PAH)$_3$ multilayers and photographic image of (CAT/PAH)$_3$/dendrimer/(dendrimer/OA−Fe_3O_4 NP)$_4$ multilayer-coated colloids displaying magnetic responsive properties. (d) Cyclic voltammograms of ITO electrode modified with the (CAT/PAH)$_3$/dendrimer/(dendrimer/OA−Fe_3O_4 NP)$_4$ multilayer-coated colloids in pH 7.0 PBS containing 15 mM H_2O_2 as a function of scan rate.

590 nm (Figure 7b). In addition, the resultant colloids were strongly affected by an external magnetic field because of the OA−Fe_3O_4 NP layers beneath the DMAP−Au_{NP} multilayers (Figure 7c). We also investigated the possibility of phase transferring the water-dispersible colloids with magnetic and metallic properties back to the organic phase. To explore this possibility, a dendrimer layer was adsorbed onto the outermost DMAP−Au_{NP} layer-coated colloids (i.e., SiO_2/(dendrimer/OA−Fe_3O_4 NP)$_4$/dendrimer/(PAA/DMAP−Au_{NP})$_2$) in an ethanol solvent (Figure 6d). It was reported that DMAP ligands are readily detached from the Au_{NP} surface due to the high affinity existing between amine groups of dendrimer and Au_{NP}.[54] Then the OA−Fe_3O_4 NPs were consecutively deposited onto the colloids via ligand exchange-induced LbL assembly in a toluene solvent. The resultant colloids (i.e., SiO_2/(dendrimer/OA−Fe_3O_4 NP)$_4$/dendrimer/(PAA/DMAP−Au_{NP})$_2$/(dendrimer/OA−Fe_3O_4 NP)$_2$ multilayer) exhibited the high dispersion stability of functional colloids in nonpolar solvent such as toluene or hexane. It should be noted here that these behaviors allowing reversible phase transfer are very useful in various applications including magnetically separable catalyst or magnetic resonance imaging (MRI). Notably, our approach can be effectively applied to a variety of hydrophobic NPs, including OA- or TOA−metal NPs (see Supporting Information, Figures S8 and S9) and OA-stabilized transition metal oxide NPs, such as OA−Fe_3O_4 NPs. TOA−metal NPs dispersed in toluene can be deposited onto dendrimer-coated colloids because of the high binding energy between the primary amine group and the metal NPs, which is similar to the ligand exchange reaction between the dendrimer and the OA−Fe_3O_4 NP. In the case of (dendrimer/TOA−Au_{NP})$_n$ multilayer-coated colloids, these colloids exhibited a highly protuberant surface structure, which led to dense surface coverage of the TOA−Au_{NP} layers as the bilayer number (n) was increased from 1 to 7 (see Supporting Information, Figure S9). Furthermore, as previously mentioned, when these colloids are coated with an outermost dendrimer layer, they can be well dispersed in aqueous media. These investigations demonstrate that our approach can be used to significantly improve the functionality of colloids to widen the range of their potential

dx.doi.org/10.1021/cm400207d | *Chem. Mater.* 2013, 25, 1735−1743

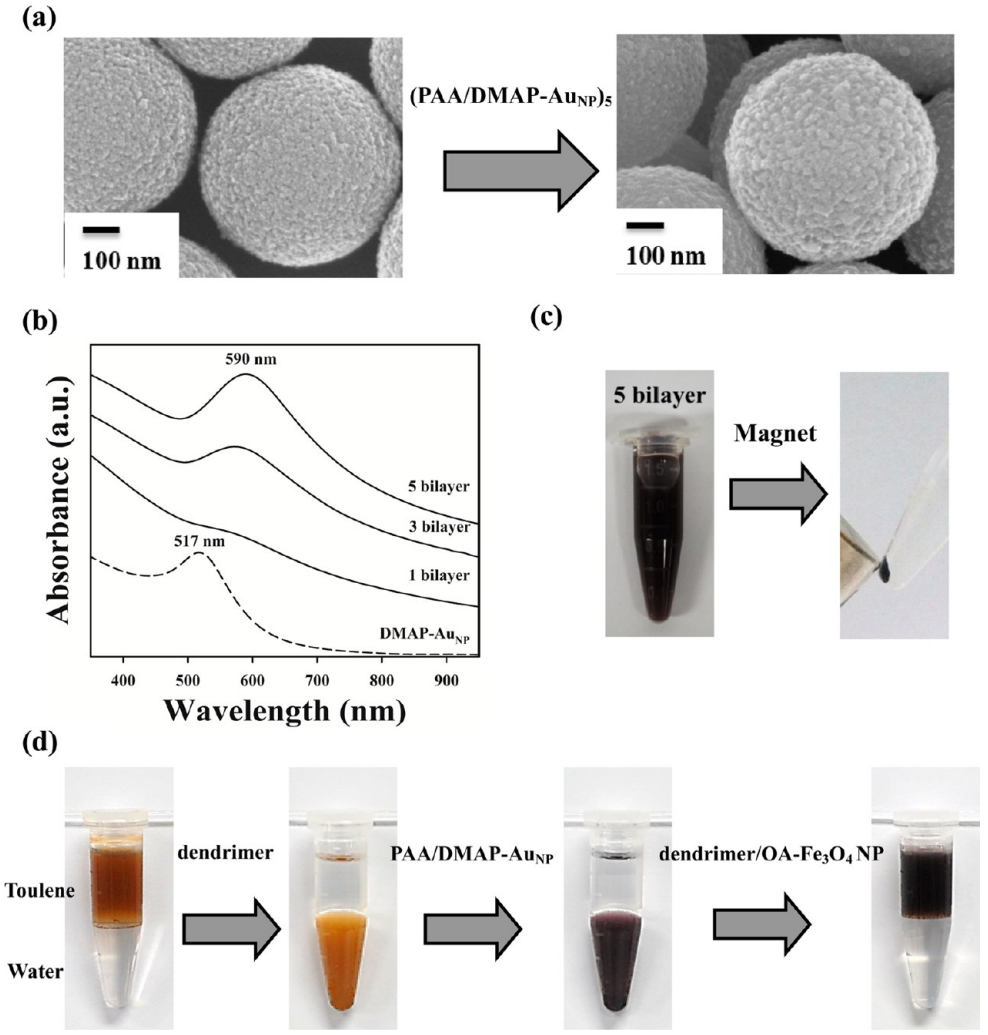

Figure 7. (a) SEM images of SiO_2 colloids/(dendrimer/OA−Fe_3O_4 NP)$_4$ (left) and SiO_2 colloids/(dendrimer/OA−Fe_3O_4 NP)$_4$/dendrimer/(PAA/DMAP−Au$_{NP}$)$_5$ (right). (b) Surface plasmon resonance spectra of SiO_2 colloids/(dendrimer/OA−Fe_3O_4 NP)$_{4.5}$/(PAA/DMAP−Au$_{NP}$)$_n$ with increasing bilayer number (n) from 1 to 5. The dotted line indicates the surface resonance spectrum of DMAP−Au$_{NP}$ in aqueous solution. (c) Photographic image of the (dendrimer/OA−Fe_3O_4 NP)$_{4.5}$/(PAA/DMAP−Au NP)$_n$ multilayer-coated colloids coated with magnetic responsive properties. (d) Photographic images of (dendrimer/OA−Fe_3O_4 NP)$_2$, (dendrimer/OA−Fe_3O_4 NP)$_2$/dendrimer, (dendrimer/OA−Fe_3O_4 NP)$_4$/dendrimer/(PAA/DMAP−Au$_{NP}$)$_2$, (dendrimer/OA−Fe_3O_4 NP)$_4$/dendrimer/(PAA/DMAP−Au$_{NP}$)$_2$/(dendrimer/OA−Fe_3O_4 NP)$_2$ multilayer-coated colloids (from left to right).

applications and to enable the reversible phase transfer of functionality integrated colloids via the easy integration of hydrophobic and hydrophilic multilayers.

CONCLUSIONS

We demonstrated that multifunctional colloids coated with hydrophobic multilayers [i.e., (dendrimer/OA−Fe_3O_4 NP)$_n$] and with electrostatic multilayers [*i.e.*, (CAT/PAH)$_n$ or (PAA/DMAP−Au$_{NP}$)$_n$] could be successfully prepared using a ligand exchange-induced, electrostatic LbL assembly method. The most important aspect of our study is that the functionality of the colloids can be easily tailored and integrated using the advantages of hydrophobic (i.e., ligand exchange-induced) and hydrophilic (i.e., electrostatic) LbL assembly. This study also demonstrates that our approach is effective for the preparation of functional colloids and enables reversible phase transfer in environments milder than those of previous approaches reported by other research groups. These multifunctional colloids can be widely used in numerous applications, such as catalysis, sensing, and optical guides, irrespective of the type of solvent used because a variety of hydrophobic metal or metal oxide NPs (e.g., OA−Ag or TOA−Au) can be used instead of OA−Fe_3O_4 NPs. We believe that our approach provides a basis for the design and exploitation of high-performance multifunctional colloids in a variety of solvents.

ASSOCIATED CONTENT

Supporting Information

TEM images of nanoparticles, photographic images, FT-IR, QCM, magnetic, SEM images, and zeta-potential curves of multilayer-coated substrates. This material is available free of charge via the Internet at http://pubs.acs.org/.

AUTHOR INFORMATION

Corresponding Author

*E-mail: jinhan71@korea.ac.kr; jungkyu_choi@korea.ac.kr.

Notes

The authors declare no competing financial interest.

■ ACKNOWLEDGMENTS

This work was supported by the National Research Foundation (NRF) grant funded by the Korea government (MEST) (2010-0029106) and ERC Program of NRF grant funded by the Korea government (MEST) (R11-2005-048-00000-0)

■ REFERENCES

(1) Decher, G. *Science* **1997**, *277*, 1232−1237.
(2) Caruso, F.; Caruso, R. A.; Möhwald, H. *Science* **1998**, *282*, 1111−1114.
(3) Tang, Z. Y.; Kotov, N. A.; Magonov, S.; Ozturk, B. *Nat. Mater.* **2003**, *2*, 413−418.
(4) Lee, B.; Kim, Y.; Lee, S.; Kim, Y. S.; Wang, D.; Cho, J. *Angew. Chem., Int. Ed.* **2010**, *49*, 359−363.
(5) Cho, J. H.; Hong, J. K.; Char, K.; Caruso, F. *J. Am. Chem. Soc.* **2006**, *128*, 9935−9942.
(6) Lee, S. W.; Kim, B.-S.; Chen, S.; Shao-Horn, Y.; Hammond, P. T. *J. Am. Chem. Soc.* **2009**, *131*, 671−679.
(7) Kim, Y.; Lee, C.; Shim, I.; Wang, D.; Cho, J. *Adv. Mater.* **2010**, *22*, 5140−5144.
(8) Dubas, S. T.; Farhat, T. R.; Schlenoff, J. B. *J. Am. Chem. Soc.* **2001**, *123*, 5368−5369.
(9) Cho, J.; Char, K.; Hong, J.-D.; Lee, K.-B. *Adv. Mater.* **2001**, *13*, 1076−1078.
(10) Cho, J.; Quinn, J. F.; Caruso, F. *J. Am. Chem. Soc.* **2004**, *126*, 2270−2271.
(11) Lee, S.; Lee, B.; Kim, B. J.; Park, J.; Bae, W. K.; Char, K.; Hawker, C. J.; Bang, J.; Cho, J. *J. Am. Chem. Soc.* **2009**, *131*, 2579−2587.
(12) Ko, Y.; Kim, Y.; Baek, H.; Cho, J. *ACS Nano* **2011**, *5*, 9918−9926.
(13) Koo, B.; Baek, H.; Cho, J. *Chem. Mater.* **2012**, *24*, 1091−1099.
(14) Renggli, K.; Baumann, P.; Langowska, K.; Onaca, O.; Bruns, N.; Meier, W. *Adv. Funct. Mater.* **2011**, *7*, 1241−1259.
(15) Wang, D.; Li, J.; Chan, C. T.; Salgueiriño-Maceira, V.; Liz-Marzán, L. M.; Romanov, S.; Caruso, F. *Small* **2005**, *1*, 122−130.
(16) Liang, Z.; Susha, A. S.; Caruso, F. *Adv. Mater.* **2002**, *14*, 1160−1164.
(17) Wang, D.; Rogach, A. J.; Caruso, F. *Chem. Mater.* **2003**, *15*, 2724−2729.
(18) Kuncicky, D. M.; Prevo, B. G.; Velev, O. D. *J. Mater. Chem.* **2006**, *16*, 1207−1211.
(19) Caruso, F.; Schüler, C. *Langmuir* **2000**, *16*, 9595−9603.
(20) Wang, D.; Rogach, A. L.; Caruso, F. *Nano Lett.* **2002**, *2*, 857−861.
(21) Dokoutchaev, A.; James, J. T.; Koene, S. C.; Pathak, S.; Prakash, G. K. S.; Thompson, M. E. *Chem. Mater.* **1999**, *11*, 2389−2399.
(22) Schmitt, J.; Decher, G.; Dressick, W. J.; Brandow, S. L.; Geer, R. E.; Shashidhar, R.; Calvert, J. M. *Adv. Mater.* **1997**, *9*, 61−65.
(23) Grabar, K. C.; Allison, K. J.; Baker, B. E.; Bright, R. M.; Brown, K. R.; Freeman, R. G.; Fox, A. P.; Keating, C. D.; Musick, M. D.; Natan, M. J. *Langmuir* **1996**, *12*, 2353−2361.
(24) Hong, J.; Bae, W.; Oh, S.; Lee, H.; Char, K.; Caruso, F.; Cho, J. *Adv. Mater.* **2007**, *19*, 4364−4369.
(25) Yoon, M.; Kim, Y.; Cho, J. *ACS Nano* **2011**, *5*, 5417−5426.
(26) Dinda, E.; Biswas, M.; Mandal, T. K. *J. Phys. Chem. C* **2011**, *115*, 18518−18530.
(27) Zhao, S.-Y.; Qiao, R.; Zhang, X. L.; Kang, Y. S. *J. Phys. Chem. C* **2007**, *111*, 7875−7878.
(28) Dorokhin, D.; Tomczak, N.; Han, M.; Reinhoudt, D. N.; Velders, A. H.; Vancso, G. J. *ACS Nano* **2009**, *3*, 661−667.
(29) Yuan, X.; Luo, Z.; Zhang, Q.; Zhang, X.; Zheng, Y.; Lee, J. Y.; Xie, J. *ACS Nano* **2011**, *5*, 8800−8808.
(30) Wu, Y.; Zhang, C.; Qu, X.; Liu, Z.; Yang, Z. *Langmuir* **2010**, *26*, 9442−9448.
(31) Goulet, P. J. G.; Santos, D. S.; Alvarez-Puebla, R. A.; Oliveira, O. N.; Aroca, R. *Langmuir* **2005**, *21*, 5576−5581.
(32) Zhang, F.; Srinivasan, M. P. *Langmuir* **2007**, *23*, 10102−10108.
(33) Joseph, Y.; Krasteva, N.; Besnard, I.; Guse, B.; Rosenberger, M.; Wild, U.; Knop-Gericke, A.; Schlogl, R.; Krustev, R.; Yasuda, A.; Vossmeyer, T. *Faraday Discuss.* **2004**, *125*, 77−97.
(34) Ko, Y.; Baek, H.; Kim, Y.; Yoon, M.; Cho, J. *ACS Nano* **2013**, *7*, 143−153.
(35) Aliev, F. G.; Correa-Duarte, M. A.; Mamedov, A.; Ostrander, J. W.; Giersig, M.; Liz-Marzán, L. M.; Kotov, N. A. *Adv. Mater.* **1999**, *11*, 1006−1010.
(36) Mamedov, A.; Ostrander, J.; Aliev, F.; Kotov, N. A. *Langmuir* **2000**, *16*, 3941−3949.
(37) Gittins, D. I.; Caruso, F. *Angew. Chem., Int. Ed.* **2001**, *40*, 3001−3004.
(38) Buttry, D. *Advances in Electroanalytical Chemistry: Applications of the QCM to Electrochemistry*; Marcel Dekker: New York, 1991.
(39) Sun, S. *Adv. Mater.* **2006**, *18*, 393−403.
(40) Chernyshova, I. V.; Ponnurangam, S.; Somasundaran, P. *Langmuir* **2011**, *27*, 10007−10018.
(41) Sun, S.; Murray, C. B.; Weller, D.; Folks, L.; Moser, A. *Science* **2000**, *287*, 1989−1992.
(42) Zhang, L.; He, R.; Gu, H.-C. *Appl. Surf. Sci.* **2006**, *253*, 2611−2617.
(43) Chalasani, R.; Vasudevan, S. *J. Phys. Chem. C* **2011**, *115*, 18088−18093.
(44) Tartaj, P.; Serna, C. J. *Chem. Mater.* **2002**, *14*, 14396−4402.
(45) Park, J.; An, K.; Hwang, Y.; Park, J.-E.; Noh, H.-J.; Kim, J.-Y.; Park, J.-H.; Hwang, N.-M.; Hyeon, T. *Nat. Mater.* **2004**, *3*, 891−895.
(46) Poddar, P.; Telem-Shafir, T.; Fried, T.; Markovich, G. *Phys. Rev. B* **2002**, *66*, 060403.
(47) Choi, J.; Rubner, M. F. *Macromolecules* **2005**, *38*, 116−124.
(48) Caruso, F.; Trau, D.; Möhwald, H. *Langmuir* **2000**, *16*, 1485−1488.
(49) Yu, A.; Caruso, F. *Anal. Chem.* **2003**, *75*, 3031−3037.
(50) Park, J.; Kim, I.; Shin, H.; Kim, Y. S.; Bang, J.; Caruso, F.; Cho, J. *Adv. Mater.* **2008**, *20*, 1843−1848.
(51) Kim, S.; Kim, Y.; Ko, Y.; Cho, J. *J. Mater. Chem.* **2011**, *21*, 8008−8013.
(52) Lee, B.; Kim, S.; Cho, J. *Macromol. Res.* **2011**, *19*, 635−638.
(53) Zhang, Z.; Chouchane, S.; Magliozzo, R. S.; Rusling, J. F. *Anal. Chem.* **2002**, *74*, 163−170.
(54) Cho, J.; Caruso, F. *Chem. Mater.* **2005**, *17*, 4547−4553.